



EXTRACTION AND RECYCLING OF BATTERY MATERIALS

# Preparation of Metal Lead from Waste Lead Paste by Direct Electrochemical Reduction in NH<sub>3</sub>-NH<sub>4</sub>Cl Solution

YANGYANG FAN,<sup>1</sup> YAN LIU,<sup>1,2</sup> LIPING NIU,<sup>1</sup> XIJUN PAN,<sup>1</sup>  
WEIGUANG ZHANG,<sup>1</sup> and TING-AN ZHANG<sup>1</sup>

1.—Key Laboratory of Ecological Metallurgy of Multi-metal Intergrown Ores of Ministry of Education, Special Metallurgy and Process Engineering Institute, Northeastern University, Shenyang 110819, Liaoning, China. 2.—e-mail: liuyan@smm.neu.edu.cn

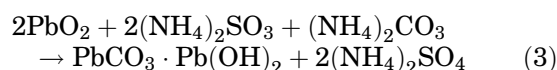
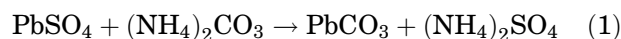
Metal lead was first prepared from waste lead paste by direct electrochemical reduction in NH<sub>3</sub>-NH<sub>4</sub>Cl solution. Cyclic voltammetry of waste lead paste powders indicated that waste lead paste could be directly electrochemically reduced to metal lead. After constant cell voltage electrolysis for 3 h, waste lead paste pellets were almost completely converted into metal containing 98.3% lead, and the current efficiency and energy consumption were approximately 86.3% and 689.4 kW h/t, respectively. In addition, an empirical model of direct electrochemical reduction of waste lead paste pellets in NH<sub>3</sub>-NH<sub>4</sub>Cl solution has been proposed. Metal lead was initially formed at a three-phase interface of the current collector, waste lead paste and electrolyte; then, the newly formed three-phase interface of the metal lead, waste lead paste and electrolyte quickly expanded along the surface of the pellets and eventually extended into the interior of the pellets.

## INTRODUCTION

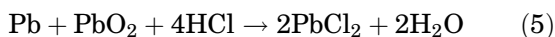
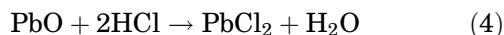
With the development of the automobile and new energy industries, an increasing number of lead acid batteries are produced each year, and waste lead acid batteries are correspondingly increasing.<sup>1</sup> Therefore, it is of great significance to recycle and deal with waste lead acid batteries economically and environmentally friendly.

The smelting process of waste lead acid batteries is much simpler than that of lead ore. As long as the reducing agent is added and the temperature reaches 1300°C, waste lead acid batteries can be reduced to metal lead.<sup>2,3</sup> Therefore, there are many factories in China that recycle and deal with lead acid batteries. However, these factories usually have a small production scale, and most use an original reverberator, cupola or crucible furnace, resulting in a low metal recovery rate, high energy consumption and poor comprehensive utilization. Most factories have no or only a small amount of simple dust collection equipment, causing a large amount of lead and sulfur dioxide fumes, which not only seriously pollute the surrounding environment of the factory but also endanger human health and waste a large amount of resources.<sup>4</sup>

Considering the environmental problems caused by traditional pyrometallurgical smelting, hydrometallurgical processes have been proposed to recover and deal with waste lead acid batteries.<sup>5–8</sup> At present, these processes chemically convert lead sulfate from waste lead paste into lead compounds that are easily electrolyzed or decomposed at a low temperature to obtain metal lead or lead oxide,<sup>9,10</sup> such as the RSR process, developed by Prengaman and McDonald,<sup>11</sup> the USBM process developed by Olper and Fracchia,<sup>12</sup> the Placid process<sup>13</sup> and the Plint process.<sup>14</sup> The lead paste from waste lead acid batteries is always desulfurized by ammonium carbonate ((NH<sub>4</sub>)<sub>2</sub>CO<sub>3</sub>) in the RSR process.<sup>11</sup> Sulfur dioxide (SO<sub>2</sub>) is also introduced to reduce lead dioxide (PbO<sub>2</sub>). The reactions in the process are as follows:



Fluoroboric acid (HBF<sub>4</sub>) or fluorosilicic acid (H<sub>2</sub>SiF<sub>6</sub>) is directly used to leach desulfurized lead paste to obtain a lead-containing solution in the USBM process.<sup>12</sup> Then, the lead-containing solution is electrodeposited to obtain metal lead, but the recovery rate of lead is low. Some researchers have also studied the Placid process based on an electrodeposition method. The lead sulfate of waste lead paste can be directly reacted with added chloride to form lead chloride.<sup>13</sup> The reactions are as follows:



On this basis, researchers have also proposed the Plint process, in which lead sulfate is dissolved in hot concentrated chloride solution to obtain electrolytic lead with a purity of more than 99.99% by electrolytic deposition.<sup>14</sup> Although these processes can prevent air pollution, there are also problems such as high energy consumption, long process flow, and large equipment investment. Therefore, the development of technologies with good economic and social benefits is still the main task of future research in the process of dealing with waste lead paste.

In this paper, metal lead was prepared from waste lead paste pellets by direct electrochemical reduction in NH<sub>3</sub>-NH<sub>4</sub>Cl solution for the first time. The electrochemical behavior of waste lead paste to metal lead was analyzed by cyclic voltammetry. Constant cell voltage electrolysis was carried out at a cell voltage of 2.30 V and at 25°C, and the growth process and macroscopic and microscopic morphologies of the metal lead from the different electrolysis stages were studied. Finally, an empirical model of the direct electrochemical reduction of solid waste lead paste pellets into metal lead in NH<sub>3</sub>-NH<sub>4</sub>Cl solution has been proposed.

## MATERIALS AND METHODS

### Materials

Experiments were carried out using simulated lead paste, which was based on a related reference, in which the proportion of each component was basically the same as the actual waste lead paste.<sup>15,16</sup> Certain proportions of lead sulfate, lead oxide, lead dioxide, lead and microcrystalline cellulose were mixed in a mixer for 2 h and then dried in a vacuum atmosphere for use. The added microcrystalline cellulose was used as a binder with a mass fraction of only 1%. The chemicals used in the experiments were all analytically pure, and the solutions were prepared using deionized water. The chemical composition of the simulated lead paste is shown in Table I.

**Table I. Chemical composition of the simulated lead paste**

Phases	PbSO <sub>4</sub>	PbO <sub>2</sub>	PbO	Pb	other
Content (wt.%)	56.43	29.70	8.91	3.96	1.00

### Electrochemical Measurements

The electrochemical measurements in NH<sub>3</sub>-NH<sub>4</sub>Cl solution were carried out using a Zennium Pro electrochemical workstation (Zahner, Germany). The cyclic voltammetry analysis used a three-electrode cell, as shown in Fig. 1a. A Pt microelectrode (100 μm diameter) was used as the working electrode. The Pt microelectrode was etched with hot aqua regia for 20 min before the experiment, forming a cavity at its tip, followed by cleaning successively with deionized water, acetone and deionized water in an ultrasonic bath. After vacuum drying, waste lead paste powders were filled into the cavity at the top of the microelectrode to obtain a Pt microelectrode filled with waste lead paste powders. The above experimental procedure was repeated again after each experiment.

### Constant Cell Voltage Electrolysis Experiments

Approximately 0.925 g of the mixed powders was weighed, placed in a powder-compressing machine, and pressed into cylindrical pellets with a diameter of 13 mm and a thickness of 1.5 mm at 12 MPa. A waste lead paste pellet was tied to a stainless steel cathode with cotton thread, and then the cathode was inserted into the electrolyte solution. An IrRu-coated Ti mesh was used as the anode, and the electrode distance was fixed at 9 mm, as shown in Fig. 1b. The pH of the ammonium chloride (NH<sub>4</sub>Cl) solution was adjusted to 7.5 with ammonium hydroxide (NH<sub>3</sub>·H<sub>2</sub>O) before the experiment, followed by electrolysis at a constant cell voltage (2.30 V). After the electrolysis was finished, the pellets were cleaned with deionized water, vacuum-dried, and analyzed. The current efficiency and energy consumption could be calculated according to the following equation:<sup>17</sup>

$$\eta = \frac{G}{qItN} \times 100\% \quad (7)$$

$$W = \frac{zFU \times 1000}{\eta M \times 3600} \quad (8)$$

where  $\eta$  is the current efficiency,  $G$  is the quality of reduced metal lead in g,  $q$  is the electrochemical equivalent of metal lead, 3.865 g/(A h),  $I$  is the current value in the electrolysis process,  $A$ ,  $t$  is the electrolysis time in h,  $N$  is the number of electrolytic cells,  $W$  is the energy consumption in kW h/t,  $z$  is

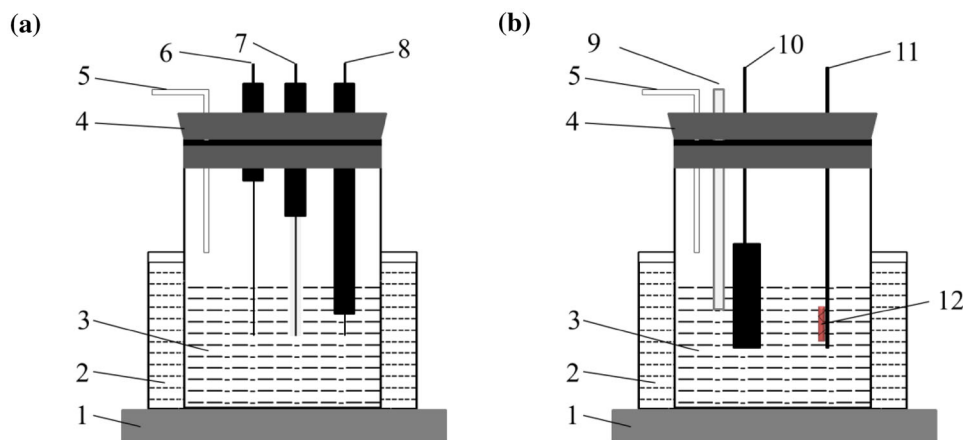


Fig. 1. Schematics of three-electrode system (a) and constant cell voltage electrolysis experiments (b); 1 heater; 2 water; 3 electrolyte; 4 plug; 5 outlet port; 6 Ag-AgCl reference electrode; 7 Pt microelectrode; 8 Pt counter electrode; 9 pH meter; 10 Ti mesh anode; 11 stainless steel cathode; 12 waste lead paste pellet.

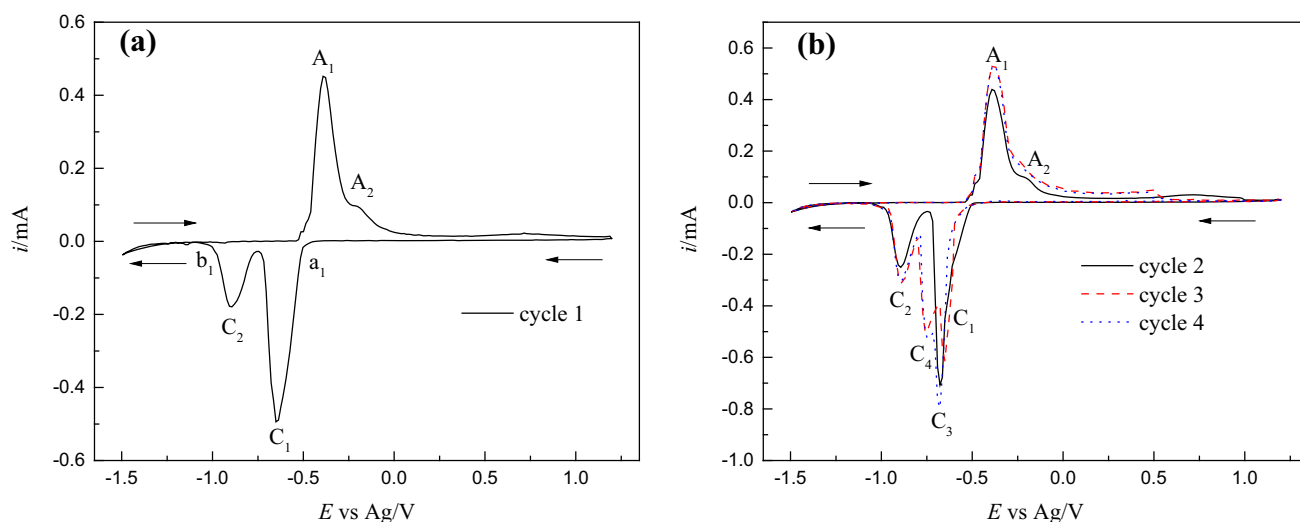


Fig. 2. Cyclic voltammety curves of waste lead paste powders in  $\text{NH}_3\text{-NH}_4\text{Cl}$  solution (temperature:  $25^\circ\text{C}$ ;  $\text{NH}_4\text{Cl}$  concentration: 2.0 mol/L; scan rate: 100 mV/s); (a) first potential cycle; (b) second to fourth potential cycles.

the number of transferred electrons,  $F$  is the Faraday constant, 96,485 C/mol,  $U$  is the cell voltage in V, and  $M$  is the molecular weight of metal lead in g/mol.

## RESULTS AND DISCUSSION

### Cyclic Voltammety

To investigate whether metal lead can be prepared from waste lead paste by direct electrochemical reduction in  $\text{NH}_3\text{-NH}_4\text{Cl}$  solution, cyclic voltammety was used in this system, as shown in Fig. 2. In Fig. 2a, the cyclic voltammety curve of waste lead paste powders in  $\text{NH}_3\text{-NH}_4\text{Cl}$  solution is shown to have started at +1.20 V, scanned in the negative direction. When the potential was scanned to point  $a_1$  (-0.53 V), the current began to increase rapidly, which indicates that metal lead

began to form by direct electrochemical reduction. There were two reduction peaks,  $C_1$  (-0.65 V) and  $C_2$  (-0.89 V), in the negative direction scan, which can be attributed to the reduction of  $\text{PbO}_2$  to  $\text{PbO}$  and subsequent reduction, producing metal lead. When the potential was scanned to point  $b_1$  (-0.96 V), the cathode current dropped rapidly to zero, indicating that the reduction process of the waste lead paste eventually stopped. When the potential was scanned through -1.50 V, the current was converted from the cathode current to the anode current. There was a distinct oxidation peak in the positive scan, corresponding to the oxidative dissolution of reduced metal lead.

Since the direct reduction rate of waste lead paste was slow at the beginning of the reaction, successive scans were performed again after the first cyclic voltammety scan, as shown in Fig. 2b. The general characteristics of the cyclic voltammety curves

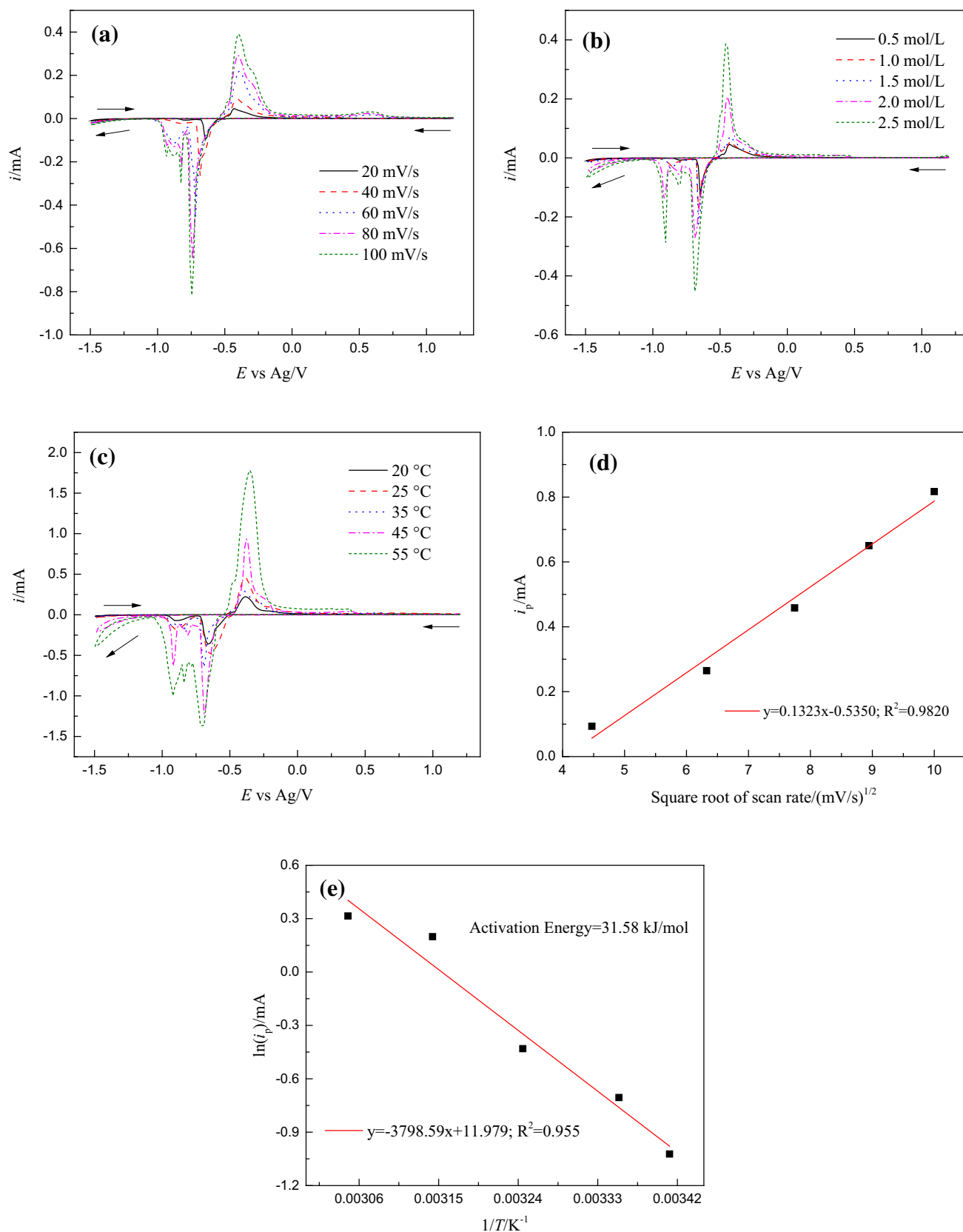


Fig. 3. Cyclic voltammograms of waste lead paste powders in  $\text{NH}_3\text{-NH}_4\text{Cl}$  solution: (a)  $25^\circ\text{C}$ ,  $0.5 \text{ mol/L}$ ; (b)  $25^\circ\text{C}$ ,  $20 \text{ mV/s}$ ; (c)  $2.0 \text{ mol/L}$ ,  $100 \text{ mV/s}$ ; the relationship between the cathodic peak current and the square root of the scan rate (d), and Arrhenius plots showing the relationship between the cathodic peak current and the temperature (e).

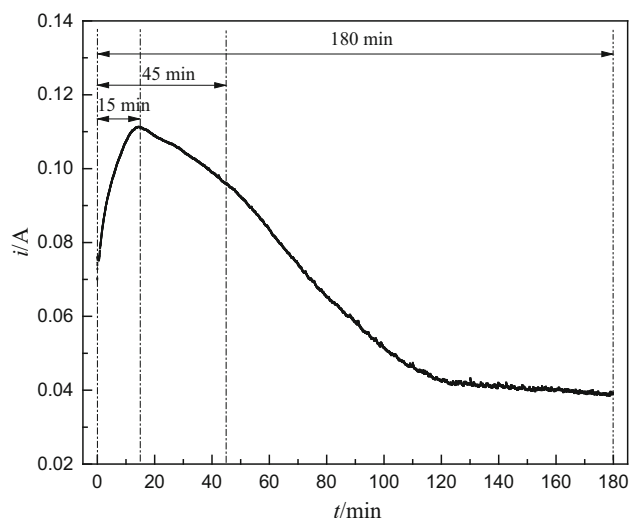
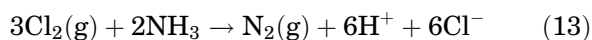
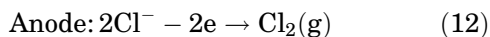
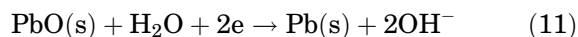
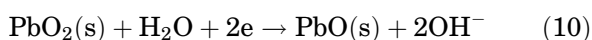
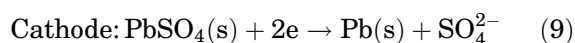


Fig. 4. The  $i$ - $t$  curve of direct electrochemical reduction in  $\text{NH}_3$ - $\text{NH}_4\text{Cl}$  solution (cell voltage: 2.30 V;  $\text{NH}_4\text{Cl}$  concentration: 2.0 mol/L; temperature: 25°C).

between the first cycle and following cycles are nearly the same except for the appearance of the reduction peaks  $C_3$  (−0.68 V) and  $C_4$  (−0.76 V) in the following cycles.  $C_3$  can be attributed to the reduction of  $\text{PbSO}_4$  to metal lead, and  $C_4$  may be caused by the existence of a transition phase of lead paste reduction. Since the lead sulfate content in the lead paste is greater than 50%, the following study focuses on the  $C_3$  peak in the direct electrochemical reduction process of lead paste. In addition, the anode released  $\text{Cl}_2$  at a certain voltage, which could react with the  $\text{NH}_3$ - $\text{NH}_4\text{Cl}$  solution to produce some  $\text{N}_2$  and chloride. This complicated the oxidation process of cyclic voltammetry, which was consistent with the fluctuation of the anode current during multiple scans (Fig. 2b). Thus, the direct reduction of waste lead paste could be expressed as:



The cyclic voltammetry curves for different scanning rates (20 mV/s, 40 mV/s, 60 mV/s, 80 mV/s, and 100 mV/s), a temperature of 25°C, and an  $\text{NH}_4\text{Cl}$  concentration of 0.5 mol/L are shown in Fig. 3a. As the scanning rate increased, the initial reduction potential remained substantially unchanged because the scanning rate had less influence on the reduction potential. However, the current of the cathodic peak gradually increased, and the corresponding current of the anodic peak also increased. Since it is of great importance to

study the control steps of direct electrochemical reduction, the peak current ( $i_p$ ) shown in Fig. 3a can be expressed by Eq. (14) according to the classic Randles–Sevcik equation.<sup>18</sup>

$$i_p = 2.69 \times 10^5 \times n^{3/2} \times A \times D^{1/2} \times C \times v^{1/2} \quad (14)$$

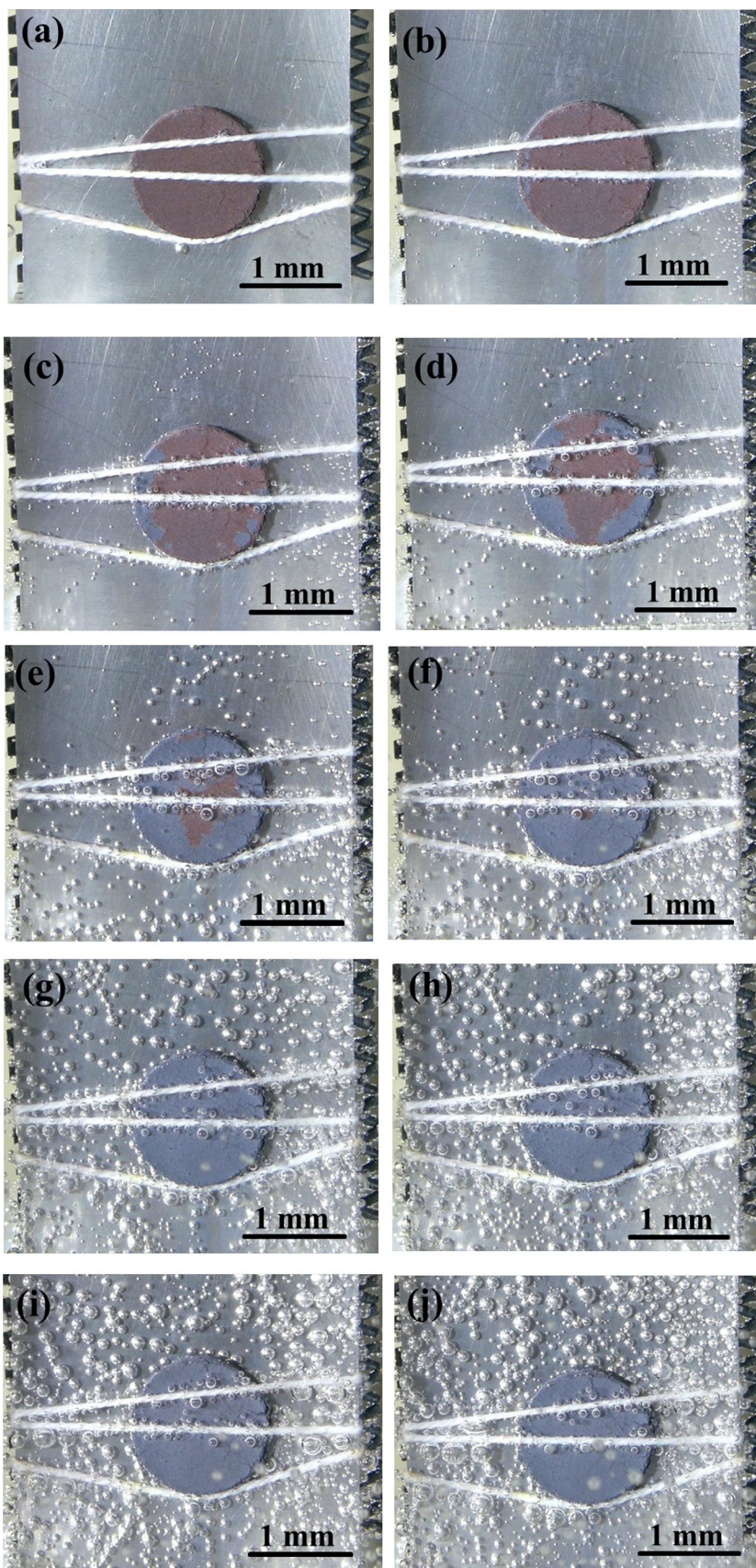
where  $n$  is the number of electrons transferred,  $A$  is the electrode area,  $D$  is the diffusion coefficient,  $C$  is the reactant concentration, and  $n$  is the scan rate. For these experiments,  $n$ ,  $A$  and  $C$  are assumed to remain unchanged; then, the diffusion coefficient ( $D$ ) depends only on the slope of  $i_p$  versus  $v^{1/2}$  according to Eq. (14). The relationship between the cathodic peak current ( $i_p$ ) and the square root of the scan rate ( $v^{1/2}$ ) is obtained, as shown in Fig. 3d. There is a good linear relationship between  $i_p$  and  $v^{1/2}$  in Fig. 3d, indicating that the direct electrochemical reduction reaction of lead paste is controlled by mass transfer. The cyclic voltammetry curves for different  $\text{NH}_4\text{Cl}$  concentrations (0.5 mol/L, 1.0 mol/L, 1.5 mol/L, 2.0 mol/L, and 2.5 mol/L), a temperature of 25°C, and a scanning rate of 20 mV/s are presented in Fig. 3b. The cathodic and anodic peak currents increased with increasing  $\text{NH}_4\text{Cl}$  concentration, and the initial reduction potential remained constant. The cyclic voltammetry curves for different temperatures (20°C, 25°C, 35°C, 45°C, and 55°C), an  $\text{NH}_4\text{Cl}$  concentration of 2.0 mol/L and a scanning rate of 100 mV/s are shown in Fig. 3c. As the temperature increased, the initial reduction potential of lead remained substantially unchanged, but the cathodic peak current increased sharply. The higher the temperature, the more obvious this phenomenon, indicating that the elevated temperature accelerated the reaction rate, which was consistent with reported conclusions.<sup>19</sup> According to the Arrhenius equation, the peak current ( $i_p$ ) shown in Fig. 3c can be expressed by Eq. (15).<sup>20</sup>

$$i_p = A \exp\left(\frac{-E_a}{RT}\right) \quad (15)$$

where  $A$  is the frequency factor,  $E_a$  is the activation energy,  $R$  is the ideal gas constant, and  $T$  is the absolute temperature. The values of  $\ln i_p$  were plotted against  $1/T$  to obtain an Arrhenius plot, as shown in Fig. 3e. This plot shows that there was a good linear relationship between  $\ln i_p$  and  $1/T$ , and the activation energy calculated by Eq. (15) was 31.58 kJ/mol, further indicating that the direct electrochemical reduction reaction of lead paste was determined by mass transfer control.

### Constant Cell Voltage Electrolysis

To further understand the reduction process, direct electrochemical reduction of waste lead paste pellets in  $\text{NH}_3$ - $\text{NH}_4\text{Cl}$  solution at 25°C and 2.30 V was carried out for 180 min. The current ( $i$ )-time ( $t$ ) curve of direct electrochemical reduction of waste lead paste pellets is shown in Fig. 4. The current



◀ Fig. 5. Optical photographs of waste lead paste pellet after electrolysis in  $\text{NH}_3\text{-NH}_4\text{Cl}$  solution with different reaction times (cell voltage: 2.30 V;  $\text{NH}_4\text{Cl}$  concentration: 2.0 mol/L; temperature: 25°C): (a) 0 min; (b) 10 min; (c) 20 min; (d) 30 min; (e) 40 min; (f) 50 min; (g) 60 min; (h) 90 min; (i) 120 min; (j) 180 min.

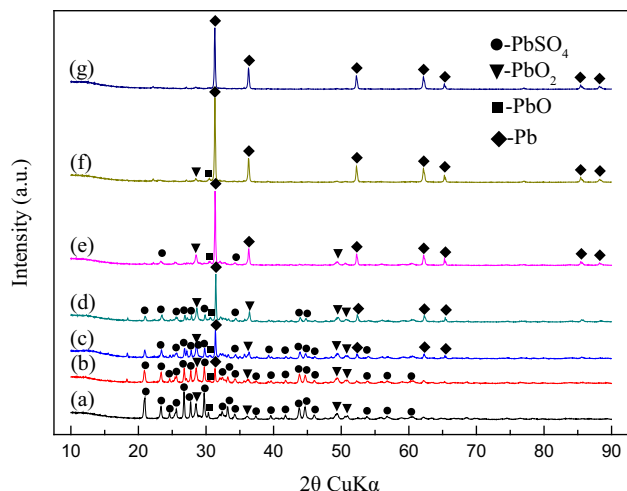


Fig. 6. XRD profiles of waste lead paste pellets after electrolysis in  $\text{NH}_3\text{-NH}_4\text{Cl}$  solution with different reaction times (cell voltage: 2.30 V;  $\text{NH}_4\text{Cl}$  concentration: 2.0 mol/L; temperature: 25°C): (a) 0 min; (b) 20 min; (c) 40 min; (d) 60 min; (e) 90 min; (f) 130 min; (g) 180 min.

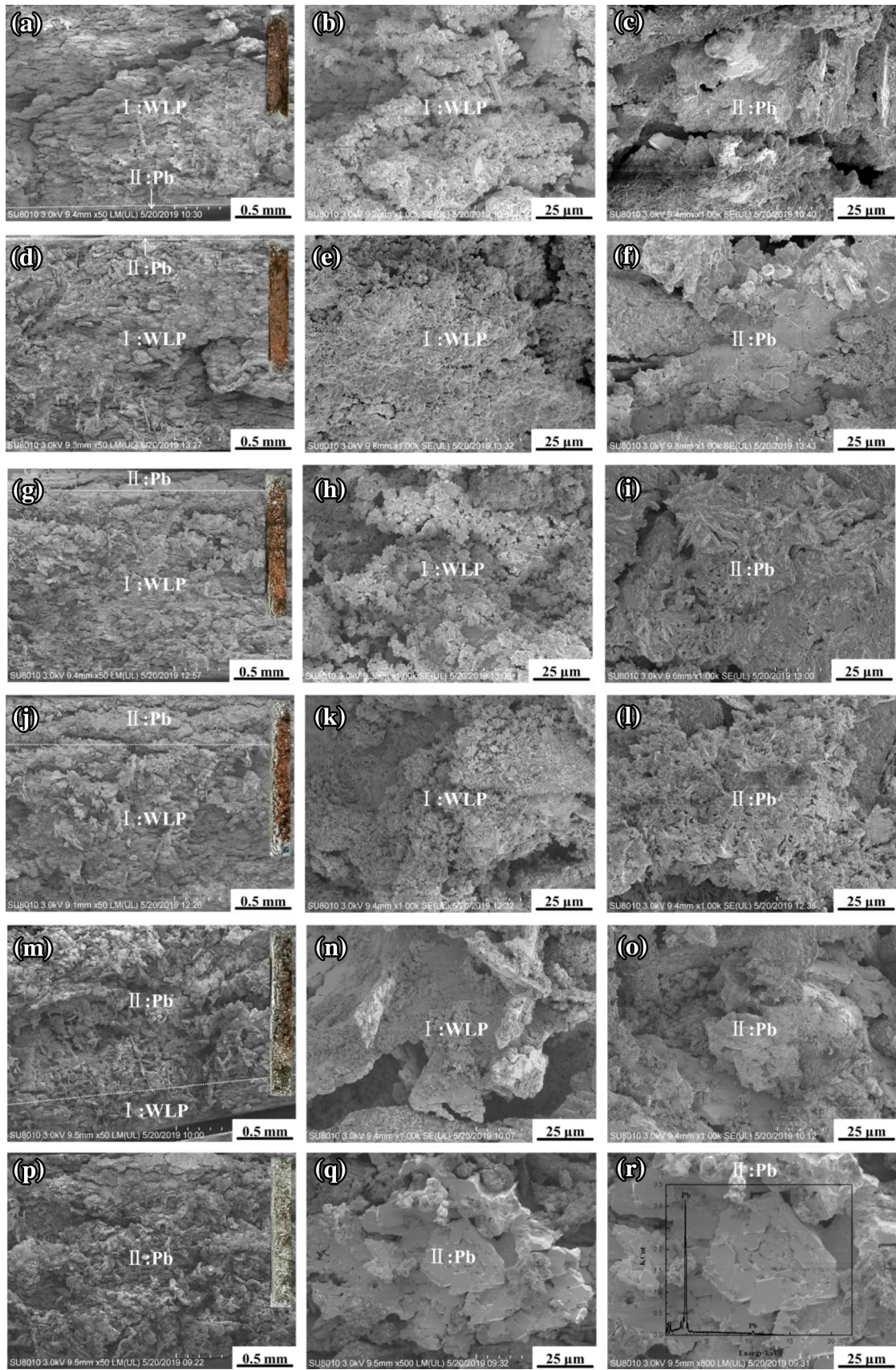
rapidly increased at the beginning of the reduction reaction and reached a maximum value of 0.111 A after 15 min. Then, the current began to slowly drop, but the current remained relatively large for 45 min, after which the current dropped significantly until it was maintained at only approximately 0.039 A after 180 min. After the electrolysis was completed, the pellets were chemically analyzed and contained 98.3% metal lead, and the current efficiency and energy consumption were approximately 86.3% and 689.4 kW h/t, respectively. Compared with the Placid or Plint processes with a high energy consumption of 1300 kW h/t, direct electrochemical reduction is more advantageous in terms of energy consumption.<sup>21</sup> Optical photographs of the corresponding reduction process are shown in Fig. 5. When the reaction time was 0 min, the waste lead paste pellet before electrolysis was reddish brown in the electrolytic cell. After 10 min of reaction, a small metallic gray color was observed on the surface of the pellet, which was reduced metal lead. As the reaction time was extended to 50 min, the surface of the pellet was almost entirely covered with metallic gray. As shown in Fig. 5, the metal lead was initially reduced on three-phase interface of the current collector, waste lead paste pellet and electrolyte. The reduced metal lead acted as a new conductive medium, forming a new three-phase interface and expanding along the surface of the pellet, which caused the current to increase rapidly with the reaction time

(Fig. 4). When the three-phase interface expanded to a maximum on the surface of the pellet, the reddish brown surface of waste lead paste pellet was almost completely covered by metallic gray color, which caused the current to continue at a relatively high value (Fig. 4). Then, the three-phase interface was finally extended in the depth direction of waste lead paste pellet, and the electrolyte diffusion became increasingly difficult, corresponding to a sharp decrease in current for the next 130 min (Fig. 4). Therefore, Fig. 5g, h, i and j shows that the size and number of bubbles on the cathode plate changed significantly, while the pellet itself did not change.

### Characterization of Waste Lead Paste and Lead Product

XRD profiles of waste lead paste pellets after electrolysis in  $\text{NH}_3\text{-NH}_4\text{Cl}$  solution with different reaction times are shown in Fig. 6. In Fig. 6a, only a few weak peaks ascribed to metal lead (Pb) can be seen; lead sulfate ( $\text{PbSO}_4$ ), lead oxide (PbO) and lead dioxide ( $\text{PbO}_2$ ) were the principal phases in the initial waste lead paste, which were in accordance with the chemical composition analysis shown in Table I. As shown in Fig. 6b, c, d, e, f and g, as the electrolysis time was prolonged, the characteristic peak of metal lead gradually increased, while the diffraction peaks of other phases continued to weaken or even disappear, such as lead sulfate ( $\text{PbSO}_4$ ), lead oxide (PbO) and lead dioxide ( $\text{PbO}_2$ ). After 180 min of electrolysis, only the characteristic peak of metal lead was observed, indicating that the extension of time was beneficial for the electrochemical reduction of waste lead paste.

SEM images of waste lead paste pellets after electrolysis in  $\text{NH}_3\text{-NH}_4\text{Cl}$  solution with different reaction times are shown in Fig. 7. To better understand the extent of reduction, the waste lead paste pellets were cut radially, as shown in the inset of Fig. 7, where area I is the waste lead paste (WLP) and area II is the metal lead (Pb). As shown in Fig. 7a, only a small portion of waste lead paste at the edge was reduced to metal lead in the initial stage of the reaction, and the interior of the pellet was not reduced. As the reaction time was extended to 60 min, the surface of the pellet was gradually reduced, but only a very thin layer inside the pellet was reduced. Additionally, fine and irregular flakes were observed. When the reaction time was 90 min, the reduction amount of waste lead paste increased, corresponding to the results shown in Fig. 5, in which the three-phase interface extended to the inside of the pellet. Figure 7m shows that, when the reaction time was extended to 130 min, most of the pellet was reduced to metal lead, but a small part of the center of the pellet was not reduced. The waste lead paste pellet was completely reduced to metal lead when the reaction time reached 180 min. In addition, the EDS pattern of Fig. 7r indicates that





◀ Fig. 7. SEM images of waste lead paste pellets after electrolysis in  $\text{NH}_3\text{-NH}_4\text{Cl}$  solution with different reaction times (cell voltage: 2.30 V;  $\text{NH}_4\text{Cl}$  concentration: 2.0 mol/L; temperature: 25°C): (a) 20 min; (b) and (c): local enlarged image (a); (d) 40 min; (e) and (f): local enlarged image (d); (g) 60 min; (h) and (i): local enlarged image (g); (j) 90 min; (k) and (l): local enlarged image (j); (m) 130 min; (n) and (o): local enlarged image (m); (p) 180 min; (q) and (r): local enlarged image (p) and the EDS spectrum measured over the image area.

only lead was present in this region. Granules and crystals could be clearly observed, and were considered to be typical precursors for metal lead.

### Analysis of the Direct Electrochemical Reduction Process

Based on the results shown in Figs. 4–7 and relevant research,<sup>17,22,23</sup> an empirical model of direct electrochemical reduction of waste lead paste pellets in  $\text{NH}_3\text{-NH}_4\text{Cl}$  solution was proposed. Therefore, the preparation process of metal lead from waste lead paste by direct electrochemical reduction in  $\text{NH}_3\text{-NH}_4\text{Cl}$  solution can be divided into three stages as follows:

1. At the beginning of the reaction, the electrolyte diffused to the side edge of waste lead paste pellet, thereby forming a three-phase interface of the current collector, waste lead paste pellet and electrolyte in this position, while the metal lead was first reduced at the interface.
2. As the reduced amount of waste lead paste gradually increased, the newly generated metal lead became the conductive medium, and the three-phase interface continuously expanded along the surface of the pellet until it was completely covered.
3. As the reaction gradually extended toward the depth direction (inside) of the pellet, the reaction efficiency significantly decreased, which might be attributed to the diffusion of the electrolyte from the metallized surface to the inside and the anion generated by the electrolysis from the inside of the pellet to the electrolyte solution.

According to the above analysis, the direct electrochemical reduction process of waste lead paste was limited to the third stage. Therefore, the reaction efficiency could be improved from the two aspects of the thickness and porosity of pellets. Apparently, the thickness of the pellet is the distance of the electrolyte diffusion, while the porosity provides passages for the electrolyte from the outside to the inside. Thus, reducing the thickness and increasing the porosity is positive for the complete diffusion of the electrolyte to form a good conductive network in pellets.

## CONCLUSION

We have demonstrated for the first time that waste lead paste can be used to prepare metal lead by direct electrochemical reduction in  $\text{NH}_3\text{-NH}_4\text{Cl}$  solution. The feasibility of direct electrochemical reduction of waste lead paste powders to metal lead was verified by cyclic voltammetry. After 180 min of constant cell voltage electrolysis at 25°C, waste lead paste pellets were reduced to metal containing 98.3% lead, in which the current efficiency and energy consumption were approximately 86.3% and 689.4 kW h/t, respectively. In addition, an empirical model of direct electrochemical reduction of waste lead paste pellets in  $\text{NH}_3\text{-NH}_4\text{Cl}$  solution was proposed. The complete penetration of the electrolyte into waste lead paste pellets to form a good conductive network is a key factor in the direct electrochemical reduction process.

## ACKNOWLEDGEMENTS

This study was financially supported by the National Natural Science Foundation of China (Grant Numbers U1760120, 51504059); the National Key R&D Program of China (Grant Numbers 2017YFC0210403-04, 2017YFC0210404); the Fundamental Research Funds for the Central Universities (Grant Numbers N162504016, N182504018); the Fund of Liaoning S&T Project (Grant Number 20180551008).

## REFERENCES

1. X. Tian, Y. Gong, Y.F. Wu, A. Agyeiwaa, and T.Y. Zuo, *Res. Conserv. Recycl.* 93, 75 (2014).
2. E.R. Cole, A.Y. Lee, and D.L. Paulson, *JOM* 35, 42 (1983).
3. E.R. Cole, A.Y. Lee, and D.L. Paulson, *JOM* 37, 79 (1985).
4. C.S. Chen, Y.J. Shi, and Y.H. Huang, *Waste Manag.* 52, 212 (2016).
5. D. Andrews, A. Raychaudhuri, and C. Frias, *J. Power Sources* 88, 124 (2000).
6. N.K. Lyakov, D.A. Atanasova, V.S. Vassilev, and G.A. Haralampiev, *J. Power Sources* 171, 960 (2007).
7. Y.J. Ma and K.Q. Qiu, *Waste Manag.* 40, 151 (2015).
8. J.Q. Pan, C. Zhang, Y.Z. Sun, Z.H. Wang, and Y.S. Yang, *Electrochem. Commun.* 19, 70 (2012).
9. J.K. Yang, X.F. Zhu, and R. Vasant Kumar, *Mater. Chem. Phys.* 131, 336 (2011).
10. X.F. Zhu, X. He, J.K. Yang, L.X. Gao, J.W. Liu, D.N. Yang, X.J. Sun, W. Zhang, Q. Wang, and R. Vasant Kumar, *J. Hazard. Mater.* 250–251, 387 (2013).
11. R.D. Prengaman, *JOM* 47, 31 (1995).
12. M. Olper, and P. Fracchia, US Patent, 4769116 (1998).
13. G. Díaz and D. Andrews, *JOM* 48, 29 (1996).
14. D. Andrews, A. Raychaudhuri, and C. Frias, *J. Power Sources* 88, 124 (2000).
15. J. Yang, J.F. Ma, Y.Y. Liu, J.C. Ma, and S.R. Batten, *Inorgan. Chem.* 46, 42 (2007).
16. R. V. Kumar, M. S. Sonmez, and V. P. Kotzeva, UK Patent, 0622249.1 (2006).
17. J.J. Ru, Y.X. Hua, C.Y. Xu, J. Li, Y. Li, D. Wang, Z.R. Zhou, and K. Gong, *Appl. Surf. Sci.* 357, 2094 (2015).
18. E. Shangguan, J. Li, D. Guo, L.T. Guo, M.Z. Nie, Z.R. Chang, X.Z. Yuan, and H.J. Wang, *J. Power Sources* 282, 158 (2015).

19. X.Y. Zhang, Y.X. Hua, C.Y. Xua, N. Xu, and H. Xue, *Electrochim. Acta* 63, 197 (2012).
20. Y.Y. Chen, U.T. Hong, H.C. Shih, J.W. Yeh, and T. Duval, *Corros. Sci.* 47, 2679 (2005).
21. G. Díaz and D. Andrews, *JOM* 48, 29 (1996).
22. W. Xiao, X.B. Jin, Y. Deng, D.H. Wang, and G.Z. Chen, *J. Electroanal. Chem.* 639, 130 (2010).
23. J.J. Ru, Y.X. Hua, D. Wang, C.Y. Xu, J. Li, Y. Li, Z.R. Zhou, and K. Gong, *Electrochim. Acta* 186, 455 (2015).

**Publisher's Note** Springer Nature remains neutral with regard to jurisdictional claims in published maps and institutional affiliations.